

Phase structure of finite temperature QCD in the heavy quark regionH. Saito,¹ S. Ejiri,² S. Aoki,^{1,3} T. Hatsuda,^{4,5,6} K. Kanaya,¹ Y. Maezawa,⁷ H. Ohno,^{1,*} and T. Umeda⁸

(WHOT-QCD Collaboration)

¹*Graduate School of Pure and Applied Sciences, University of Tsukuba, Tsukuba, Ibaraki 305-8571, Japan*²*Graduate School of Science and Technology, Niigata University, Niigata 950-2181, Japan*³*Center for Computational Sciences, University of Tsukuba, Tsukuba, Ibaraki 305-8577, Japan*⁴*Department of Physics, The University of Tokyo, Tokyo 113-0033, Japan*⁵*IPMU, The University of Tokyo, Kashiwa 277-8583, Japan*⁶*Theoretical Research Division, Nishina Center, RIKEN, Wako 351-0198, Japan*⁷*Mathematical Physics Laboratory, Nishina Center, RIKEN, Wako 351-0198, Japan*⁸*Graduate School of Education, Hiroshima University, Hiroshima 739-8524, Japan*

(Received 6 June 2011; published 8 September 2011)

We study the quark mass dependence of the finite temperature QCD phase transition in the heavy quark region using an effective potential defined through the probability distribution function of the average plaquette. Performing a simulation of SU(3) pure gauge theory, we first confirm that the distribution function has two peaks indicating that the phase transition is of first order in the heavy quark limit, while the first-order transition turns into a crossover as the quark mass decreases from infinity, where the mass dependence of the distribution function is evaluated by the reweighting method combined with the hopping parameter expansion. We determine the endpoint of the first-order transition region for $N_f = 1, 2, 3$ and $2 + 1$ cases. The quark mass dependence of the latent heat is also evaluated in the first-order transition region.

DOI: 10.1103/PhysRevD.84.054502

PACS numbers: 12.38.Gc, 11.15.Ha, 12.38.Mh

I. INTRODUCTION

The QCD phase transition is one of the important ingredients in understanding the evolution of the early universe. Monte Carlo simulation of lattice QCD is the most powerful approach to study the nature of the QCD phase transition at present [1]. It is known that the order of the phase transition depends on the values of quark masses: The deconfinement phase transition is of first order when masses of all three (up, down, and strange) quarks are either sufficiently large or small, while it turns into a crossover in the intermediate region [2–7]. Previous studies with staggered quarks strongly suggest that the transition becomes a crossover at physical quark masses [8–10]. A confirmation of this result by other fermion formulations such as Wilson-type fermions or by other methods of analyses is, however, mandatory to draw a definite conclusion on the nature of the transition at physical quark masses [11–13].

Among several methods to study the nature of phase transitions, a probability distribution of physical observables provides us with the most intuitive way to determine the order of the phase transition. Adopting an appropriate physical quantity such as a quark number, chiral order parameter, gauge action etc., the corresponding probability distribution function is constructed by measuring a

generation rate of configurations at each fixed value of the physical quantity. Then an existence of double or multiple peaks in the probability distribution function give a signal of a first-order phase transition, since two phases coexist at a first-order phase transition point.

In this study, we investigate the quark mass dependence of the order of the QCD phase transition in the large quark mass region using the hopping parameter expansion. We expect the first-order phase transition in the heavy quark limit becomes a crossover as we decrease the quark masses from infinity. We take the plaquette, i.e. 1×1 Wilson loop, as the quantity to study the order of the transition. The reweighting technique [14,15] is employed to vary quark masses in the lowest order of the hopping parameter expansion, and we determine an endpoint where the first-order phase transition turns into a crossover.

This paper is organized as follows. Basic properties of the plaquette distribution function are discussed in Sec. II. A method to calculate the plaquette distribution function by the hopping parameter expansion is introduced in Sec. III. Details of our simulations and results for the effective potential defined from the distribution function are presented in Sec. IV. Results show that the first-order phase transition becomes a crossover as the quark mass decreases from infinity. We then determine the location of the endpoint for the cases of $N_f = 1, 2, 3$ and $2 + 1$ with the Wilson quark action. Our conclusions are given in Sec. VI.

*Present address: Physics Department, Brookhaven National Laboratory, Upton, NY 11973, USA.

II. PROBABILITY DISTRIBUTION FUNCTION

A probability distribution function provides us with one of the most powerful methods to determine the order of phase transitions. Since there exist two phases simultaneously at a first-order phase transition point, we expect that the probability distribution function has multiple peaks near the transition point. In this study, we consider the distribution function of the average plaquette P ,

$$P = \frac{1}{6N_{\text{site}}} \sum_{n,\mu < \nu} \frac{1}{3} \text{Re tr}[U_{n,\mu} U_{n+\hat{\mu},\nu} U_{n+\hat{\nu},\mu}^\dagger U_{n,\nu}^\dagger], \quad (1)$$

where $U_{n,\mu}$ is the link variable and $N_{\text{site}} = N_s^3 \times N_t$ is the lattice volume. We adopt the standard one-plaquette action (S_g) for glues and the standard Wilson fermion action (S_q) for quarks:

$$S_g = -6N_{\text{site}}\beta P, \quad (2)$$

$$S_q = \sum_{f=1}^{N_f} \left\{ \sum_n \bar{\psi}_n^{(f)} \psi_n^{(f)} - \kappa_f \sum_{n,\mu} \bar{\psi}_n^{(f)} [(1 - \gamma_\mu) U_{n,\mu} \psi_{n+\hat{\mu}}^{(f)} + (1 + \gamma_\mu) U_{n-\hat{\mu},\mu}^\dagger \psi_{n-\hat{\mu}}^{(f)}] \right\} \quad (3)$$

$$\equiv \sum_{f=1}^{N_f} \left\{ \sum_{n,m} \bar{\psi}_n^{(f)} M_{nm}(\kappa_f) \psi_m^{(f)} \right\}, \quad (4)$$

where N_f is the number of flavors, κ_f is the hopping parameter for the f -th flavor, and $\beta = 6/g^2$ is the (inverse) gauge coupling. The hopping parameter κ_f controls the quark mass, which is proportional to $1/\kappa_f$ for small κ_f , while the lattice spacing is mainly controlled by β . For the case of degenerate quark masses, i.e. $\kappa_f = \kappa$ for $f = 1, \dots, N_f$, the plaquette distribution function is defined as

$$w(P', \beta, \kappa) = \int \mathcal{D}U \mathcal{D}\psi \mathcal{D}\bar{\psi} \delta(P' - P) e^{-S_q - S_g} \\ = \int \mathcal{D}U \delta(P' - P) (\det M(\kappa))^{N_f} e^{6\beta N_{\text{site}} P}. \quad (5)$$

The partition function is given by $Z(\kappa, \beta) = \int w(P', \beta, \kappa) dP'$. In the followings, we denote the argument P' in w simply as P .

The plaquette distribution function has the following useful property [15]. Under the change from β_0 to β , $w(P, \beta, \kappa)$ transforms as

$$w(P, \beta, \kappa) = e^{6(\beta - \beta_0)N_{\text{site}}P} w(P, \beta_0, \kappa). \quad (6)$$

Therefore, the effective potential defined by

$$V_{\text{eff}}(P, \beta, \kappa) = -\ln w(P, \beta, \kappa) \quad (7)$$

transforms as

$$V_{\text{eff}}(P, \beta, \kappa) = V_{\text{eff}}(P, \beta_0, \kappa) - 6(\beta - \beta_0)N_{\text{site}}P. \quad (8)$$

From this property, we find that

$$\frac{dV_{\text{eff}}}{dP}(P, \beta, \kappa) = \frac{dV_{\text{eff}}}{dP}(P, \beta_0, \kappa) - 6(\beta - \beta_0)N_{\text{site}}, \quad (9)$$

and d^2V_{eff}/dP^2 is independent of β .

Since the distribution function is doubly peaked at and around a first-order transition point, the corresponding effective potential has a double-well structure and the derivative dV_{eff}/dP becomes an S-shaped function. Therefore, close to the transition point, dV_{eff}/dP must vanish at three points. In general, to find the first-order phase transition by observing these properties, a fine-tuning of β is required. For the case of the plaquette effective potential, however, we can detect the existence of the first-order transition through the appearance of the S-shape in dV_{eff}/dP without fine tunings, since the P -dependence of dV_{eff}/dP itself is independent of β as shown in Eq. (9). After the detection, the first-order transition region in β , in which dV_{eff}/dP vanishes at three values of P , can be identified using Eq. (9). Therefore, dV_{eff}/dP is useful to determine a region of the first-order phase transition.

We next discuss the κ -dependence of V_{eff} considering the ratio of the distribution functions at κ and κ_0 :

$$R(P', \kappa, \kappa_0) \equiv \frac{w(P', \beta, \kappa)}{w(P', \beta, \kappa_0)} \quad (10)$$

$$= \frac{\int \mathcal{D}U \delta(P' - P) (\det M(\kappa))^{N_f} e^{6\beta N_{\text{site}} P}}{\int \mathcal{D}U \delta(P' - P) (\det M(\kappa_0))^{N_f} e^{6\beta N_{\text{site}} P}} \\ = \frac{\int \mathcal{D}U \delta(P' - P) (\det M(\kappa))^{N_f}}{\int \mathcal{D}U \delta(P' - P) (\det M(\kappa_0))^{N_f}} \\ = \frac{\langle \delta(P' - P) \frac{(\det M(\kappa))^{N_f}}{(\det M(\kappa_0))^{N_f}} \rangle_{(\beta, \kappa_0)}}{\langle \delta(P' - P) \rangle_{(\beta, \kappa_0)}}. \quad (11)$$

Note that $R(P, \kappa, \kappa_0)$ is independent of β , and thus $R(P, \kappa, \kappa_0)$ can be evaluated at any β . Using $R(P, \kappa, \kappa_0)$, the κ -dependence of the effective potential is given by

$$V_{\text{eff}}(P, \beta, \kappa) = -\ln R(P, \kappa, \kappa_0) + V_{\text{eff}}(P, \beta, \kappa_0). \quad (12)$$

This argument can be easily generalized to improved gauge actions including larger Wilson loops, for which we redefine the average plaquette as $P = -S_g/(6N_{\text{site}}\beta)$. On the other hand, β -dependent improved quark actions make the analysis more complicated.

We note that the identification of the order of the phase transition by the V_{eff} is equivalent to that by the fourth-order Binder cumulant, $B_4 = \langle (X - \langle X \rangle)^4 \rangle / \langle (X - \langle X \rangle)^2 \rangle^2$ with X an appropriate operator signaling the phase transition, since both V_{eff} and B_4 detect a change of the distribution function. On the other hand, to correctly evaluate B_4 at a first-order transition point, we need to know precisely the probability distribution in a wide range of X covering both peaks [15]. A fine-tuning to the transition

point and a high statistics with sufficiently many flip-flops are required for a reliable estimate of B_4 at the transition point. Furthermore, to achieve well-separated peaks, a large system volume is required. This makes the whole study quite demanding, in particular, for weak first-order transitions such as the case of the heavy quark limit of QCD. On the other hand, a reliable V_{eff} in a wide range of P can be easily obtained by combining data at different β points thanks to the relation (8).

III. QUARK DETERMINANT IN THE HEAVY QUARK REGION

To investigate the quark mass dependence of the plaquette effective potential, we evaluate the quark determinant by a Taylor expansion with respect to the hopping parameter κ in the vicinity of the simulation point κ_0 :

$$\begin{aligned} \ln \left[\frac{\det M(\kappa)}{\det M(\kappa_0)} \right] &= \sum_{n=1}^{\infty} \frac{1}{n!} \left[\frac{\partial^n (\ln \det M)}{\partial \kappa^n} \right]_{\kappa_0} (\kappa - \kappa_0)^n \\ &= \sum_{n=1}^{\infty} \frac{\mathcal{D}_n}{n!} (\kappa - \kappa_0)^n, \end{aligned} \quad (13)$$

where

$$\begin{aligned} \mathcal{D}_n &\equiv \left[\frac{\partial^n \ln \det M}{\partial \kappa^n} \right]_{\kappa_0} \\ &= (-1)^{n+1} (n-1)! \text{tr} \left[\left(M^{-1} \frac{\partial M}{\partial \kappa} \right)^n \right]_{\kappa_0}. \end{aligned} \quad (14)$$

Calculating the derivative of the quark determinant \mathcal{D}_n , the κ -dependence of the effective potential can be estimated.

Adopting $\kappa_0 = 0$, the Eq. (14) reads

$$\mathcal{D}_n = (-1)^{n+1} (n-1)! \text{tr} \left[\left(\frac{\partial M}{\partial \kappa} \right)^n \right]_{\kappa=0}, \quad (15)$$

where $M_{x,y} = \delta_{x,y}$ at $\kappa = 0$. and $(\partial M / \partial \kappa)_{x,y}$ is the gauge connection between x and y . Therefore, the non-vanishing contributions to \mathcal{D}_n are given by Wilson loops or Polyakov loops. Considering the antiperiodic boundary condition and gamma matrices in the hopping terms, the leading-order contributions to the Taylor expansion are given by

$$\begin{aligned} \ln \left[\frac{\det M(\kappa)}{\det M(0)} \right] &= 288 N_{\text{site}} \kappa^4 P + 12 \times 2^{N_t} N_s^3 \kappa^{N_t} \text{Re} \Omega \\ &+ \dots, \end{aligned} \quad (16)$$

where Ω is the Polyakov loop defined by

$$\Omega = \frac{1}{N_s^3} \sum_{\mathbf{n}} \frac{1}{3} \text{tr} [U_{\mathbf{n},4} U_{\mathbf{n}+\hat{4},4} U_{\mathbf{n}+2\hat{4},4} \dots U_{\mathbf{n}+(N_t-1)\hat{4},4}]. \quad (17)$$

The ratio $R(P, \kappa, 0) = w(P, \beta, \kappa) / w(P, \beta, 0)$ is then calculated at arbitrary values of β but small κ as follows.

$$\begin{aligned} R(P', \kappa, 0) &= \frac{\langle \delta(P' - P) \exp[N_f (288 N_{\text{site}} \kappa^4 P + 12 \times 2^{N_t} N_s^3 \kappa^{N_t} \text{Re} \Omega + \dots)] \rangle_{(\beta, \kappa_0=0)}}{\langle \delta(P' - P) \rangle_{(\beta, \kappa_0=0)}} \\ &= e^{288 N_f N_{\text{site}} \kappa^4 P'} \frac{\langle \delta(P' - P) \exp[N_f (12 \times 2^{N_t} N_s^3 \kappa^{N_t} \text{Re} \Omega + \dots)] \rangle_{(\beta, \kappa_0=0)}}{\langle \delta(P' - P) \rangle_{(\beta, \kappa_0=0)}}. \end{aligned} \quad (18)$$

For the case of $N_t = 4$ we study, the truncation error is $O(\kappa^6)$. The contribution from the plaquette can be absorbed by a shift of β .

IV. NUMERICAL SIMULATIONS AND THE RESULTS

A. Simulation parameters and plaquette effective potential

In the heavy quark limit we perform simulations of SU(3) pure gauge theory on a $24^3 \times 4$ lattice. We generate the configurations by a pseudo heat bath algorithm followed by four over-relaxation sweeps. We perform simulations at five β values in the range 5.68–5.70. Simulation points and statistics are summarized in Table I.

The results for the histogram of P , i.e. the plaquette distribution function Eq. (5) normalized by the partition function Z , are plotted in Fig. 1. In this calculation, we

approximate the delta function by a Gaussian function: $\delta(x) \approx 1/(\Delta\sqrt{\pi}) \exp[-(x/\Delta)^2]$, where Δ corresponds to the width of the Gaussian function. As Δ decreases, the resolution of the distribution function becomes better, while the statistical error increases. Examining the resolution and the statistical error, we adopt $\Delta = 0.000283$. This

TABLE I. The number of configurations and the bin size for jackknife error analyses.

β	configurations	bin size
5.6800	100 000	100
5.6850	430 000	2150
5.6900	500 000	2000
5.6925	670 000	3350
5.7000	100 000	500

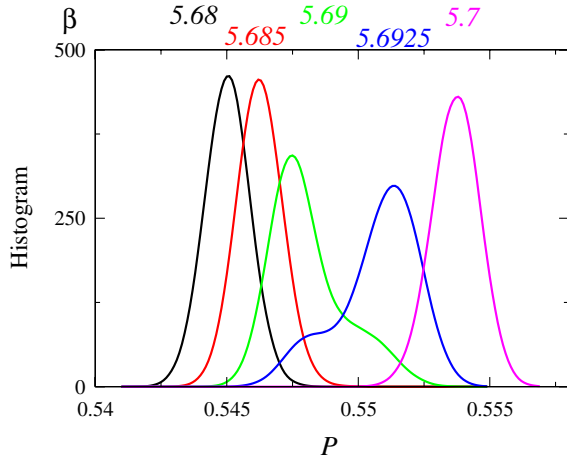


FIG. 1 (color online). Plaquette histogram w/Z obtained by SU(3) pure gauge simulations at $\beta = 5.68\text{--}5.70$ on the $24^3 \times 4$ lattice.

figure shows that the value of P generated in a simulation at single β distributes in a narrow range.

We then calculate the derivative dV_{eff}/dP by the difference between the potentials at $P - \epsilon_P/2$ and $P + \epsilon_P/2$. The value of ϵ_P is set to be 0.0001, considering the resolution in P . The ϵ_P -dependence is much smaller than the statistical error around this value of ϵ_P . Results of dV_{eff}/dP at $\kappa = 0$ are shown in Fig. 2, where data points with low statistics are removed for clarity. In this figure, we adjust results at different β 's to $\beta = 5.69$ by using Eq. (9). Results of dV_{eff}/dP obtained in simulations at different β are consistent with each other within statistical errors, though the ranges of P in which V_{eff} is reliably obtained are different. The jackknife method is used to estimate the statistical error of the effective potential and its derivatives. The bin size of the jackknife analysis is listed in Table I. We then combine these data by taking an average weighted

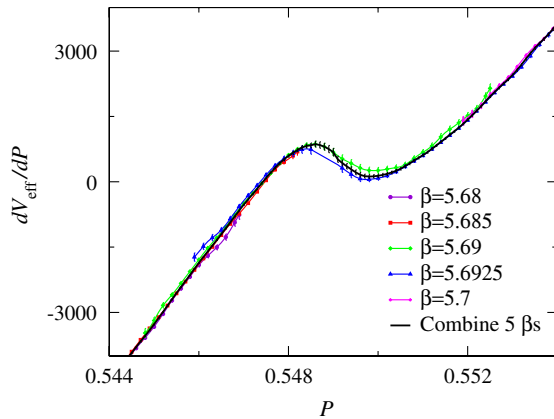


FIG. 2 (color online). Derivative of the effective potential in SU(3) pure gauge theory at $\beta = 5.69$ converting data obtained at $\beta = 5.68\text{--}5.70$ by Eq. (9). The bold black curve is an average over the results obtained at different β .

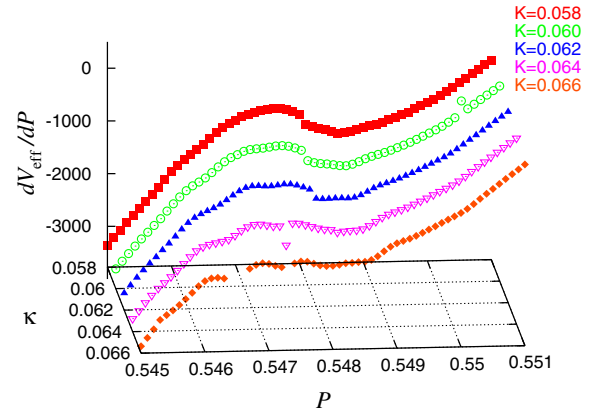


FIG. 3 (color online). Derivative of the effective potential at nonzero κ in two-flavor QCD.

with the inverse-square of errors in the overlapping regions. We here exclude data at P far away from the peak of the distribution at each β which thus has poor statistics. The final result for dV_{eff}/dP at $\kappa = 0$ is shown by the black line without symbols in Fig. 2. We find that dV_{eff}/dP is not a monotonically increasing function at $\kappa = 0$, indicating that the effective potential has a double-well shape.

The quark mass dependence of the effective potential is investigated by calculating $R(P, \kappa, 0)$ up to the order κ^4 in Eq. (18). Using the data of $w(P, \beta, \kappa = 0)$ and $R(P, \kappa, 0)$, we evaluate the dV_{eff}/dP at nonzero κ . Results for $N_f = 2$ are plotted in Fig. 3. The S-shape structure becomes weaker as κ increases and turns into a monotonically increasing function around $\kappa = 0.066$. This behavior suggests that the first-order phase transition at $\kappa = 0$ becomes weaker as κ increases and the transition becomes a cross-over at $\kappa \approx 0.066$. In Fig. 4 we show the κ dependence of V_{eff} obtained by a numerical integration of dV_{eff}/dP . In this figure, β is adjusted such that the two minima have the same height (see Sec. IV B 2 for details), and the integration is started from the peak point P_{peak} of V_{eff} between

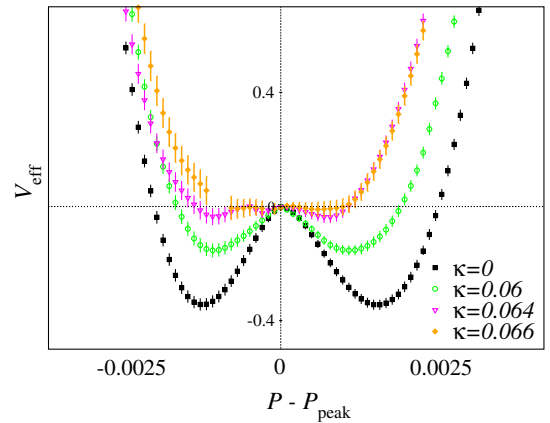


FIG. 4 (color online). Effective potential V_{eff} at β_{trans} for each κ .

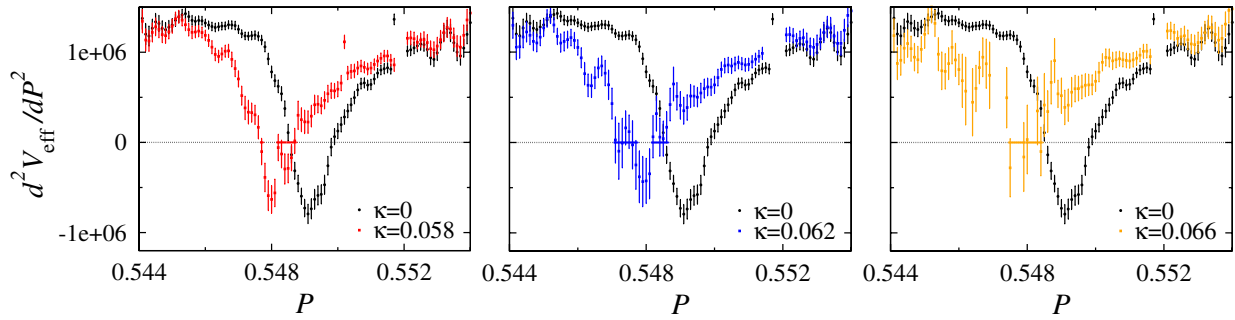


FIG. 5 (color online). Curvature of the effective potential at $\kappa = 0.058$ (left), 0.062 (middle), 0.066 (right). Black symbols are results at $\kappa = 0$. Bold horizontal lines on the line of $d^2V_{\text{eff}}/dP^2 = 0$ represent errors of the plaquette values where d^2V_{eff}/dP^2 vanish.

the two minima. We find that the double-well becomes shallower as κ increases and become almost flat around $\kappa = 0.066$.

B. Critical point in the heavy quark region for $N_f=2$

In this subsection, we evaluate the value of κ at which the first-order phase transition terminates. We denote the corresponding critical point as κ_{cp} .

1. Critical point from d^2V_{eff}/dP^2

We first calculate the second derivative of $V_{\text{eff}}(P, \beta, \kappa)$ by a numerical differentiation of dV_{eff}/dP . When the transition is of first order, there is a region in P where d^2V_{eff}/dP^2 is negative between the two bottoms of $V_{\text{eff}}(P, \beta, \kappa)$. The first-order transition region is thus identified by calculating the sign of the second derivative of V_{eff} . As discussed in Sec. II, the second derivative of $V_{\text{eff}}(P, \beta, \kappa)$ is independent of β . Therefore, the identification can be performed at any β .

In Fig. 5, we plot the results of d^2V_{eff}/dP^2 at $\kappa = 0.058$ (left), 0.062 (middle) and 0.066 (right) for $N_f = 2$, together

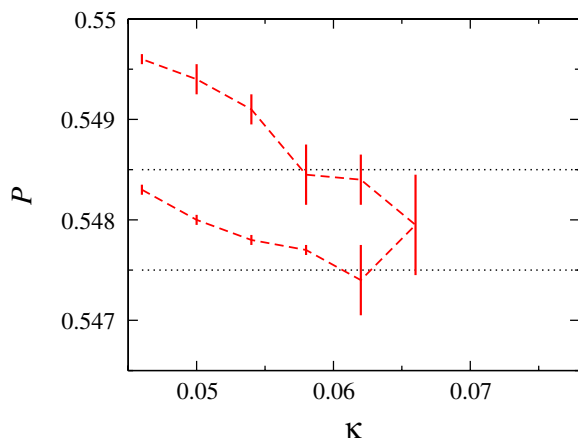


FIG. 6 (color online). Value of P where d^2V_{eff}/dP^2 vanishes at each κ .

with the results at $\kappa = 0$ which are shown as black symbols. We find that the region where $d^2V_{\text{eff}}/dP^2 < 0$ becomes narrower as κ increases. Bold horizontal lines at zero show the range of P where the curvature vanishes within statistical errors. Hereafter we denote the position at which $d^2V_{\text{eff}}/dP^2 = 0$ as $P_{(V''_{\text{eff}}=0)}(\kappa)$ or $\kappa_{(V''_{\text{eff}}=0)}(P)$. Results of $P_{(V''_{\text{eff}}=0)}$ are plotted in Fig. 6 as a function of κ . The region of the negative curvature seems to vanish around $\kappa = 0.066$. Since the curvature is always positive beyond this κ , the effective potential is no longer a double-well type, i.e. the transition becomes a crossover at $\kappa \gtrsim 0.066$.

To evaluate the critical point κ_{cp} we study the κ -dependence of d^2V_{eff}/dP^2 at fixed P , as shown in Fig. 7 for typical points. Data with large statistical errors are removed from this figure. Fitting data by a linear function in κ , we obtain $\kappa_{(V''_{\text{eff}}=0)}(P)$, which is shown by a square symbol in the same figure. The horizontal bar represents the statistical error. Results of $\kappa_{(V''_{\text{eff}}=0)}$ are plotted in Fig. 8 for $0.5474 \leq P \leq 0.5487$. When κ is larger than the maximum value of $\kappa_{(V''_{\text{eff}}=0)}$, d^2V_{eff}/dP^2 is non-negative for all values of P in this region. Therefore, the maximum value of $\kappa_{(V''_{\text{eff}}=0)}$ is nothing but the critical point κ_{cp} . We obtain $\kappa_{\text{cp}} = 0.0685(72)$ for $N_f = 2$.

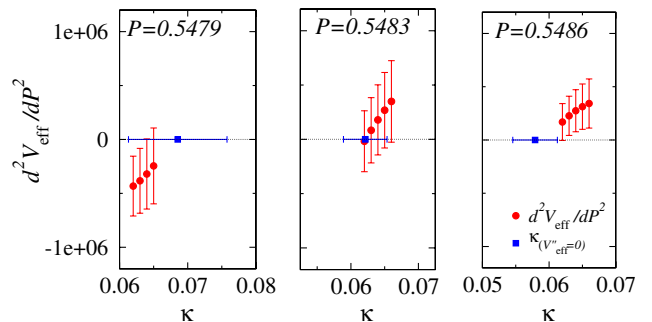


FIG. 7 (color online). κ -dependence of d^2V_{eff}/dP^2 and the results of $\kappa_{(V''_{\text{eff}}=0)}$ at $P = 0.5479, 0.5483$ and 0.5486 .

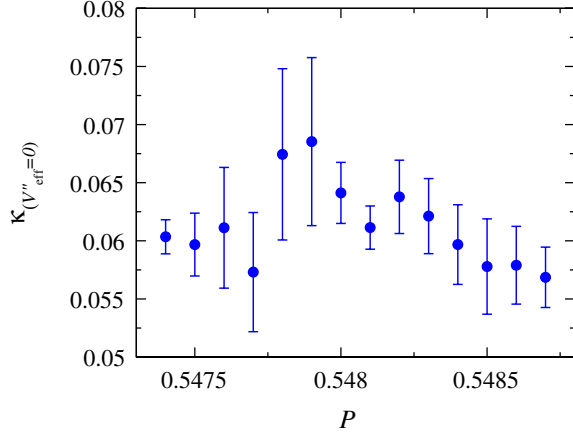


FIG. 8 (color online). Value of κ where d^2V_{eff}/dP^2 vanishes at each P .

2. Critical point from the double-well structure of V_{eff}

Alternatively, we may determine κ_{cp} as the point where the two minima of $V_{\text{eff}}(P)$ merge and the barrier between the two minima vanishes. The double-well structure of V_{eff} is most clearly seen at β where the two minima of V_{eff} has the same height (see Fig. 4). Such β , say β_{trans} , can be determined by a Maxwell's construction for dV_{eff}/dP : Let us denote the values of P at the two minima as P_A and P_B . The condition $V_{\text{eff}}(P_A) = V_{\text{eff}}(P_B)$ implies $\int_{P_A}^{P_B} \frac{dV_{\text{eff}}}{dP}(P, \beta_{\text{trans}}, \kappa) dP = 0$, or, equivalently,

$$\int_{P_A}^{P_{\text{peak}}} \frac{dV_{\text{eff}}}{dP}(P, \beta_{\text{trans}}, \kappa) dP = - \int_{P_{\text{peak}}}^{P_B} \frac{dV_{\text{eff}}}{dP}(P, \beta_{\text{trans}}, \kappa) dP \quad (19)$$

where P_{peak} is the peak position of V_{eff} between P_A and P_B at which dV_{eff}/dP vanishes. Changing β by Eq. (9), we

search β_{trans} where Eq. (19) is satisfied. The results for β_{trans} are plotted in the left panel of Fig. 9 as a function of κ . At $\kappa = 0$, we obtain $\beta_{\text{trans}} = 5.69138(3)$. At $\kappa = 0.066$, because the minima of V_{eff} are too shallow to apply the Maxwell construction, we instead determine β_{trans} as the point where the bottom region of V_{eff} becomes flat, as shown in Fig. 4. In the right pane of Fig. 9, we replot β_{trans} as a function of κ^4 , as motivated by the hopping parameter expansion. We note that the data is well fitted by a linear function of κ^4 .

In an approximation to disregard fluctuations around the plaquette expectation value P , we can identify $V_{\text{eff}}(P)$ with the free energy of the system. Then the condition $V_{\text{eff}}(P_A) = V_{\text{eff}}(P_B)$ means that the pressure p is balanced between the phases A and B. Therefore, we may view β_{trans} as an estimate of the first-order transition point. Actually, our result $\beta_{\text{trans}} = 5.69138(3)$ for $\kappa = 0$ is quite close to the first-order transition point $\beta_{\text{trans}} = 5.69153(86) - 5.69211(35)$ defined by the peak position of the plaquette susceptibility in SU(3) pure gauge theory with the same lattice size $24^3 \times 4$ [3].

In Fig. 10, results of the potential barrier height $V_{\text{peak}} \equiv V_{\text{eff}}(P_{\text{peak}}) - V_{\text{eff}}(P_A)$ and the gap $\Delta P \equiv P_B - P_A$ at β_{trans} are shown as functions of κ . We find that both V_{peak} and ΔP decrease drastically above $\kappa = 0.05$ and vanish around $\kappa \approx 0.066$. Performing a linear extrapolation using three nearest points of V_{peak} [ΔP] as shown in Fig. 10, we obtain $\kappa_{\text{cp}} = 0.0647(6)$ [0.0662(4)]. A corresponding value of β_{cp} at the critical point can be estimated by extrapolating β_{trans} to κ_{cp} , assuming a linear function in κ or κ^4 as plotted in Fig. 9. Results for κ_{cp} and β_{cp} are summarized in Table II. In the table, we also present β_{cp} for κ_{cp} determined by d^2V_{eff}/dP^2 . From these results, we obtain

$$\kappa_{\text{cp}} = 0.0658(3)_{(-11)}^{(+4)}, \quad \beta_{\text{cp}} = 5.6843(1)(4) \quad (20)$$

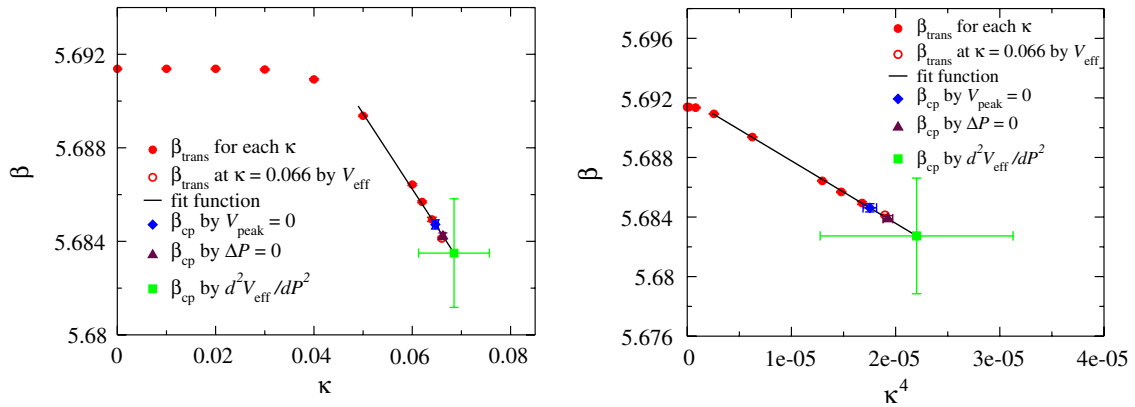


FIG. 9 (color online). β_{trans} as a function of κ (Left) and κ^4 (Right) for $N_f = 2$. Also shown are the results of the critical point (β_{cp}), which are obtained by linearly extrapolating β_{trans} in κ (Left) or κ^4 (Right) to κ_{cp} determined by V_{peak} (diamonds) or d^2V_{eff}/dP^2 (squares).

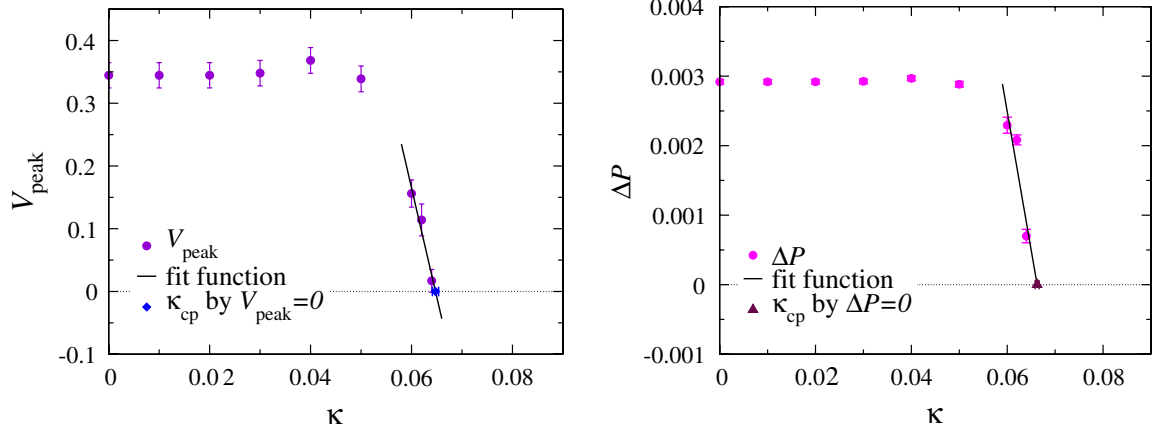


FIG. 10 (color online). Potential barrier height V_{peak} (Left) and the gap ΔP (Right) between the two minima at β_{trans} for $N_f = 2$. Critical point κ_{cp} is estimated by linear extrapolations shown in the figures.

where the central values and their statistical errors given in the first brackets are determined by a weighted average of the results, and systematic errors given in the second brackets are determined from the scattering of the results due to the method and extrapolation function, neglecting the data from the d^2V_{eff}/dP^2 method which are consistent with other results within large errors.

To get a rough idea about the value of the pseudoscalar meson mass (m_{PS}) corresponding to the critical point, we estimate the ratio $T/m_{\text{PS}} = 1/(N_t m_{\text{PS}} a)$ at the critical point. Using a data of zero-temperature pseudoscalar meson mass in $N_f = 2$ QCD along the finite temperature crossover curve for $N_t = 4$ in the range $\kappa = 0.16\text{--}0.19$ [16], we perform a fit $(m_{\text{PS}} a)^{-1} = f_1 \kappa^2 + f_2 \kappa^4$ with fitting parameters f_1 and f_2 , where the constraint $(m_{\text{PS}} a)^{-1} = 0$ at $\kappa = 0$ is taken into account. We find $T/m_{\text{PS}} \approx 0.023$ for $N_f = 2$ at the critical point $\kappa_{\text{cp}} \approx 0.066$. Because $T_{\text{trans}}/m_{\text{PS}} = O(1)$ around the physical point, the small value 0.023 means that the critical pseudoscalar meson mass is much larger than the physical pion mass.

C. Latent heat

The gap of the internal energy density, $\Delta\varepsilon$, at a first-order transition point is called the latent heat. Since p is

TABLE II. Critical point κ_{cp} and β_{cp} defined by V_{peak} , ΔP and d^2V_{eff}/dP^2 .

method	κ_{cp}	β_{cp}
	κ fit	κ^4 fit
V_{peak}	0.0647(06)	5.6847(02) 5.6846(03)
ΔP	0.0662(04)	5.6842(01) 5.6838(02)
d^2V_{eff}/dP^2	0.0685(72)	5.6834(23) 5.6827(39)
total	0.0658(3) $^{+4}_{-11}$	5.6843(1)(4)

continuous there, $\Delta\varepsilon$ can be evaluated as the gap of the trace anomaly:

$$\begin{aligned}
 \frac{\varepsilon - 3p}{T^4} &= -\frac{1}{VT^3} a \frac{d \ln Z}{da} - [T = 0] \\
 &= -N_t^4 \left[a \frac{d\beta}{da} 6\langle P \rangle + N_f a \frac{d\kappa}{da} (1152\kappa^3 \langle P \rangle \right. \\
 &\quad \left. + N_t^{-1} 12 \times 2^{N_t} \kappa^{N_t-1} \langle \text{Re}\Omega \rangle \right) + O(\kappa^6) \Big] \\
 &\quad - [T = 0]
 \end{aligned} \tag{21}$$

where $[T = 0]$ is the zero-temperature contribution to be subtracted for renormalization. At $\kappa = 0$, $(1/6)a(d\beta/da) \approx -(0.064\text{--}0.078)$ at $\beta = \beta_c(N_t = 4)$, depending on the method to define the scale [17–20]. At $\kappa = 0$, $\langle \text{Re}\Omega \rangle = 0$ due to the center $Z(3)$ symmetry, and $a(d\kappa/da) = 0$ because $\kappa = 0$ is a line of constant physics. Neglecting terms proportional to $\kappa^3 a(d\kappa/da)$ at small κ , the latent heat is roughly evaluated as

$$\frac{\Delta\varepsilon}{T^4} = \frac{\Delta(\varepsilon - 3p)}{T^4} \approx -6N_t^4 a \frac{d\beta}{da} \langle \Delta P \rangle \tag{22}$$

where ΔP is shown in Fig. 10 for $N_f = 2$. It is found from the behavior of ΔP that the latent heat decreases as κ increases.

V. THE CASES OF 2+1-FLAVOR AND DEGENERATE N_f -FLAVOR QCD

The analysis can be easily generalized to an arbitrary value of N_f and also to the case of $N_f = 2 + 1$ QCD. At the leading order of the hopping parameter expansion, the contribution of quark determinants in the partition function is given by

$$\ln \left[\frac{(\det M(\kappa_{\text{ud}}))^2 \det M(\kappa_s)}{(\det M(0))^3} \right] = 288 N_{\text{site}} (2\kappa_{\text{ud}}^4 + \kappa_s^4) P + 12 \times 2^{N_t} N_s^3 (2\kappa_{\text{ud}}^{N_t} + \kappa_s^{N_t}) \text{Re} \Omega + \dots \quad (23)$$

for the case of $N_f = 2 + 1$, where κ_{ud} and κ_s are hopping parameters for light and strange quarks. The modification factor for the reweighting in κ thus becomes

$$R(P', \kappa_{\text{ud}}, \kappa_s, 0) = e^{288 N_{\text{site}} (2\kappa_{\text{ud}}^4 + \kappa_s^4) P'} \frac{\langle \delta(P' - P) \exp[12 \times 2^{N_t} N_s^3 (2\kappa_{\text{ud}}^{N_t} + \kappa_s^{N_t}) \text{Re} \Omega + \dots] \rangle_{(\beta, \kappa=0)}}{\langle \delta(P' - P) \rangle_{(\beta, \kappa=0)}}. \quad (24)$$

Since the contribution from the plaquette in this equation does not affect the second derivative of V_{eff} , the difference from the case of $N_f = 2$ is just the replacement of $2\kappa^{N_t}$ by $2\kappa_{\text{ud}}^{N_t} + \kappa_s^{N_t}$. Thus, the line which separates the first-order phase transition and the crossover is given by

$$2(\kappa_{\text{ud}})^{N_t} + (\kappa_s)^{N_t} = 2(\kappa_{\text{cp}}^{N_f=2})^{N_t} \quad (25)$$

where $N_t = 4$ and $\kappa_{\text{cp}}^{N_f=2} = 0.0658(3)_{-11}^{+4}$ as determined in Sec. IV B. We draw the line in Fig. 11, in which the colored region corresponds to the first-order transition. The case of degenerate N_f -flavor QCD can be similarly investigated. Results for κ_{cp} are summarized in Table III for $N_f = 1, 2$ and 3. Our κ_{cp} for $N_f = 1$ is consistent with the result obtained by an effective model in Ref. [21]. In the present approximation of the lowest-order hopping parameter expansion at $N_t = 4$, β_{cp} is independent of N_f .

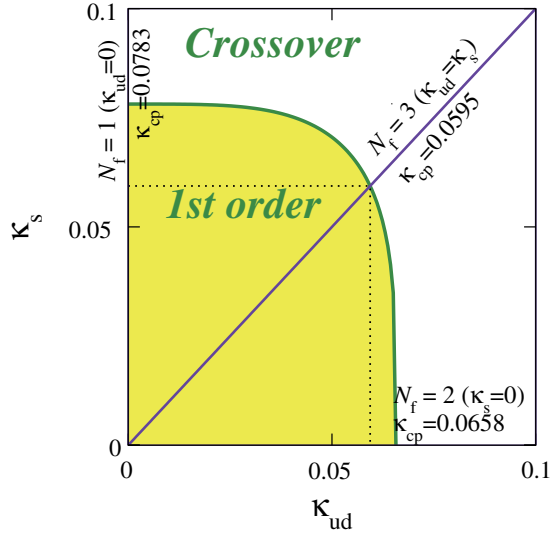


FIG. 11 (color online). The phase boundary separating the first-order transition region and crossover region in the $(\kappa_{\text{ud}}, \kappa_s)$ plane.

VI. CONCLUSION

We have investigated the order of the deconfinement phase transition in the heavy quark region of QCD by calculating an effective potential $V_{\text{eff}}(P)$ defined as the logarithms of the probability distribution function for the average plaquette P . To study the fate of the first-order deconfinement transition, V_{eff} has to be reliably evaluated in a wide range of P covering the both phases. Applying a reweighting method, we combine the results at five different β points to calculate V_{eff} in a wide range of P . We evaluate V_{eff} at $\kappa = 0$ by simulations in SU(3) pure gauge theory, and reweight it to nonzero but small values of κ using the leading-order hopping parameter expansion on an $N_t = 4$ lattice.

At $\kappa = 0$, $V_{\text{eff}}(P)$ show clear double-well structure in accordance with the first-order deconfinement transition of the SU(3) pure gauge theory. When we increase κ from zero, the double-well shape becomes weaker, and eventually disappear at finite κ , indicating that the first-order transition turns into a crossover at that point as suggested from the effective Z(3) model with an external magnetic field. We estimated the critical point κ_{cp} by examining various properties of V_{eff} . The results for the critical point in degenerate N_f -flavor QCD as well as that in the $N_f = 2 + 1$ QCD are summarized in Table III and Fig. 11.

The calculations are done in the leading-order approximation of the hopping parameter expansion on an $N_t = 4$ lattice. Although the values of κ_{cp} we obtained are quite small, it is important to confirm the reliability of the leading-order approximation quantitatively. In the next leading order, we have $O(\kappa^6)$ contributions from Wilson loops with length 6 and $O(\kappa^{N_t+2})$ contributions from Polyakov loops which have $N_t + 2$ link variables including two spatial links. To estimate the effects of them, measurement of the probability distribution function including expectation values for

TABLE III. κ_{cp} for $N_f = 1, 2$ and 3 determined by the reweighting method with the lowest-order hopping parameter expansion at $N_t = 4$.

N_f	κ_{cp}
1	$0.0783(4)_{-13}^{+5}$
2	$0.0658(3)_{-11}^{+4}$
3	$0.0595(3)_{-10}^{+4}$

these operators is required. Another important point to be studied is the continuum extrapolation by increasing N_t . We leave these studies as future works.

ACKNOWLEDGMENTS

We would like to thank Y. Taniguchi for discussions. This work is in part supported by Grants-in-Aid of the

Japanese Ministry of Education, Culture, Sports, Science and Technology (Nos. 21340049, 22740168, 22840020, 20340047, 23540295) and by the Grant-in-Aid for Scientific Research on Innovative Areas (Nos. 20105001, 20105003, 23105706). H.O. is supported by the Japan Society for the Promotion of Science for Young Scientists.

-
- [1] See, e.g., K. Yagi, T. Hatsuda, and Y. Miake, *Quark-Gluon Plasma* (Cambridge University Press, Cambridge, 2005).
- [2] R.D. Pisarski and F. Wilczek, *Phys. Rev. D* **29**, 338 (1984).
- [3] M. Fukugita, M. Okawa, and A. Ukawa, *Nucl. Phys.* **B337**, 181 (1990).
- [4] Y. Iwasaki, K. Kanaya, T. Yoshié, T. Hoshino, T. Shirakawa, Y. Oyanagi, S. Ichii, and T. Kawai, *Phys. Rev. D* **46**, 4657 (1992).
- [5] T. Banks and A. Ukawa, *Nucl. Phys.* **B225**, 145 (1983).
- [6] T.A. DeGrand and C.E. DeTar, *Nucl. Phys.* **B225**, 590 (1983).
- [7] F. Karsch, Ch. Schmidt, and S. Stickan, *Comput. Phys. Commun.* **147**, 451 (2002).
- [8] E. Laermann and O. Philipsen, *Annu. Rev. Nucl. Part. Sci.* **53**, 163 (2003).
- [9] Y. Aoki, G. Endrodi, Z. Fodor, S.D. Katz, and K.K. Szabo, *Nature (London)* **443**, 675 (2006).
- [10] S. Ejiri, F. Karsch, E. Laermann, C. Miao, S. Mukherjee, P. Petreczky, C. Schmidt, W. Soeldner, and W. Unger, *Phys. Rev. D* **80**, 094505 (2009).
- [11] Y. Iwasaki, K. Kanaya, S. Kaya, and T. Yoshie, *Phys. Rev. Lett.* **78**, 179 (1997).
- [12] A. Ali Khan *et al.* (CP-PACS Collaboration), *Phys. Rev. D* **63**, 034502 (2000); **64**, 074510 (2001).
- [13] S. Ejiri, Y. Maezawa, N. Ukita, S. Aoki, T. Hatsuda, N. Ishii, K. Kanaya, and T. Umeda (WHOT-QCD Collaboration), *Phys. Rev. D* **82**, 014508 (2010).
- [14] A.M. Ferrenberg and R.H. Swendsen, *Phys. Rev. Lett.* **61**, 2635 (1988); **63**, 1195 (1989).
- [15] S. Ejiri, *Phys. Rev. D* **77**, 014508 (2008).
- [16] K.M. Bitar *et al.*, *Phys. Rev. D* **43**, 2396 (1991).
- [17] R.G. Edwards, U.M. Heller, and T.R. Klassen, *Nucl. Phys.* **B517**, 377 (1998).
- [18] G. Boyd, J. Engels, F. Karsch, E. Laermann, C. Legeland, M. Luetgemeier, and B. Petersson, *Nucl. Phys.* **B469**, 419 (1996).
- [19] K. Akemi, M. Fujisaki, M. Okuda, Y. Tago, Ph. deForcrand, T. Hashimoto, S. Hioki, O. Miyamura, T. Takaishi, A. Nakamura, and I.O. Stamatescu, *Phys. Rev. Lett.* **71**, 3063 (1993).
- [20] S. Ejiri, Y. Iwasaki, and K. Kanaya, *Phys. Rev. D* **58**, 094505 (1998).
- [21] C. Alexandrou, A. Borici, A. Feo, P. de Forcrand, A. Galli, F. Jegerlehner, and T. Takaishi, *Phys. Rev. D* **60**, 034504 (1999).